

Research Paper

Elasto-plastic fine-scale damage failure analysis of metro structures based on coupled SBFEM-FEM

Kai Chen, Degao Zou*, Xianjing Kong, Jingmao Liu

The State Key Laboratory of Coastal and Offshore Engineering, Dalian University of Technology, Dalian, Liaoning 116024, China
 School of Hydraulic Engineering, Dalian University of Technology, Dalian, Liaoning 116024, China

ARTICLE INFO

Keywords:

Scaled boundary finite element method (SBFEM)
 Damage propagation
 Polyhedron fine-scale analysis
 Similar element technique
 DaiKai metro

ABSTRACT

This paper presents a new high-performance, fine-scale damage analysis method using three techniques. Firstly, efficient and detailed mesh discretization is performed via octree, which can easily accomplish cross scale and thus significantly alleviate the burden of fine modelling using octant cubes. Secondly, the introduction of coupled scaled boundary finite element (SBFEs) into FEM can offer more generality, flexibility and conveniences. Thirdly, the parameter matrices (e.g. stiffness, mass, damping) of geometrically similar elements generated by octree are proportionable and can be pre-computed. Therefore, by leveraging the similarity among elements for elasto-plastic problems will significantly improve computational efficiency. In order to demonstrate the effectiveness of the new approach, a fine-scale damage evolution of DaiKai subway was comprehensively modelled using different mesh sizes. Plastic damage and generalized plasticity models for soil and interfaces were used. Results from the case study demonstrated that octree possesses the advantages of high robustness, ability for automation and capacity to work with fewer elements during mesh generation. The coupled SBFEM-FEM and the use of element similarity markedly improved the computation cost (50% computation time was reduced). The presented method bypasses the need for undesired compromise between simulation accuracy and solver efficiency.

1. Introduction

With rapid urbanization in China, the living standard of the people is improving, and increasing numbers of people are able to afford and drive vehicles. However, with more population joining the transportation networks, urban congestion (e.g. traffic jams) have becoming a more prominent problem in large and medium-sized cities. One solution to improving urban congestion is to give the city population the option to travel via subway transit. By shifting a portion of city transit activity underground, urban planners gain more freedom in planning city the layout and functions. Studies [1] show that the subway is an essential tool to alleviate the pressure of urban congestion, and is central in the process of transforming a city into a modern metropolis.

While subway transit offers great benefits, cities prone to seismic activities must consider how its subway network can be damaged once an earthquake strikes. Damage to the transit system as well as the rest of the city infrastructure can be disastrous. As seen from prior major earthquakes such as the Tangshan, Taiwan Chi-Chi and Wenchuan earthquakes, heavy blows and huge economic losses were dealt to the nation. Therefore, there is great value in being able to effectively and efficiently perform reinforce against seismic damage for large underground structures, and aim to

ensure their safe and smooth operation.

In such a regard, scholars have conducted much research. Chen et al. [2–4] studied the frequency response of a model subway tunnel through shake table excitation and through numerical simulation. Uenishi et al. [5], Cao et al. [6], Huo et al. [7] analyzed the earthquake-induced damage of the DaiKai metro. Liu et al. [8], Sun et al. [9], Liu et al. [10] discussed the seismic performance of subway and underground structures. Huan et al. [11] analyzed the damage of a subway station structure through three-dimensional simulation. Zhang et al. [12] considered the effect of soil liquefaction on seismic behavior of metro structures. Gu et al. [13] introduced the three-dimensional viscoelastic boundary and also considered the scattering of seismic waves. Lu et al. [14] studied and analyzed the influence of certain soil-structure interaction characteristics on earthquake-induced damage; Du et al. [15,16] investigated the earthquake-induced failure of a subway station using nonlinear geotechnical constitutive models.

In summary, the seismic analysis of Metro structures has made a lot of research achievements, which can better serve the engineering construction. However, it is worth pointing out that the refined seismic damage analysis is still rarely reported. The main reason is the structural characteristics of the metro system itself. Generally speaking, subway systems are typically bear the following characteristics. Firstly,

* Corresponding author at: The State Key Laboratory of Coastal and Offshore Engineering, Dalian University of Technology, Dalian, Liaoning 116024, China.
 E-mail address: zoudegao@dlut.edu.cn (D. Zou).

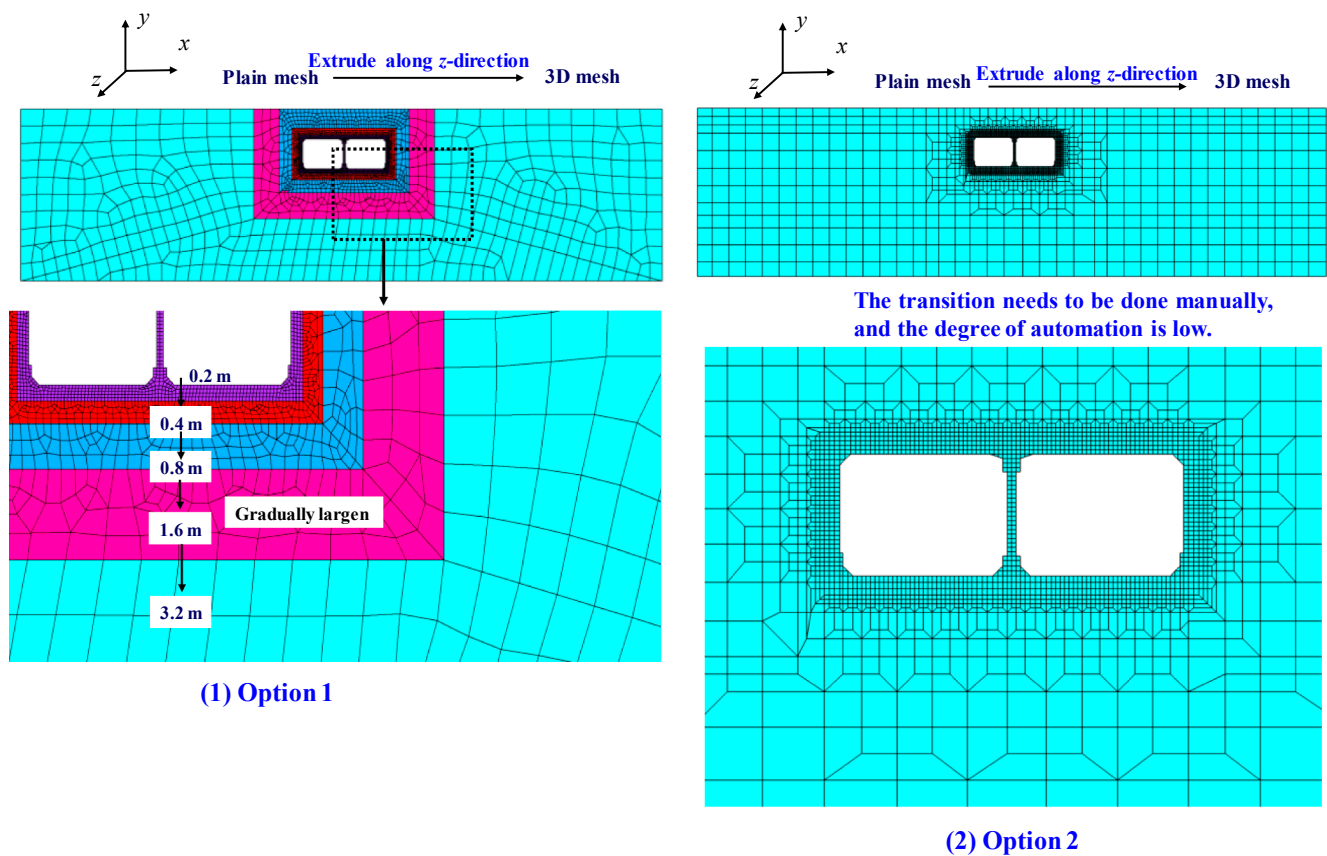


Fig. 1. Manual/semi-automatic element transition for handling structure-soil interaction.

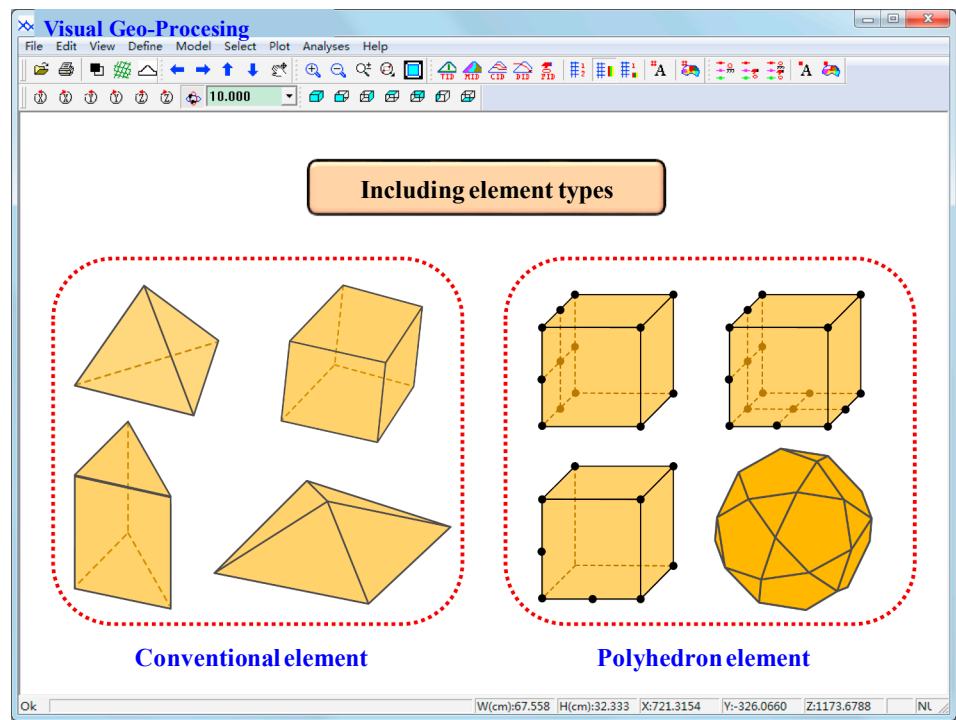


Fig. 2. Supported element types in GEODYNA.

the structural properties of the surrounding soil and concrete are quite different. Therefore, interface elements should be considered in modeling the contact of these two materials. The conventional interface element is similar to the traditional isoparametric element. The element

surface only supports triangles and quadrilateral geometries, which have higher geometrical requirements for mesh discretization. Secondly, the size difference between the structure and the soil is significant. As there will be a stress concentration in the concrete

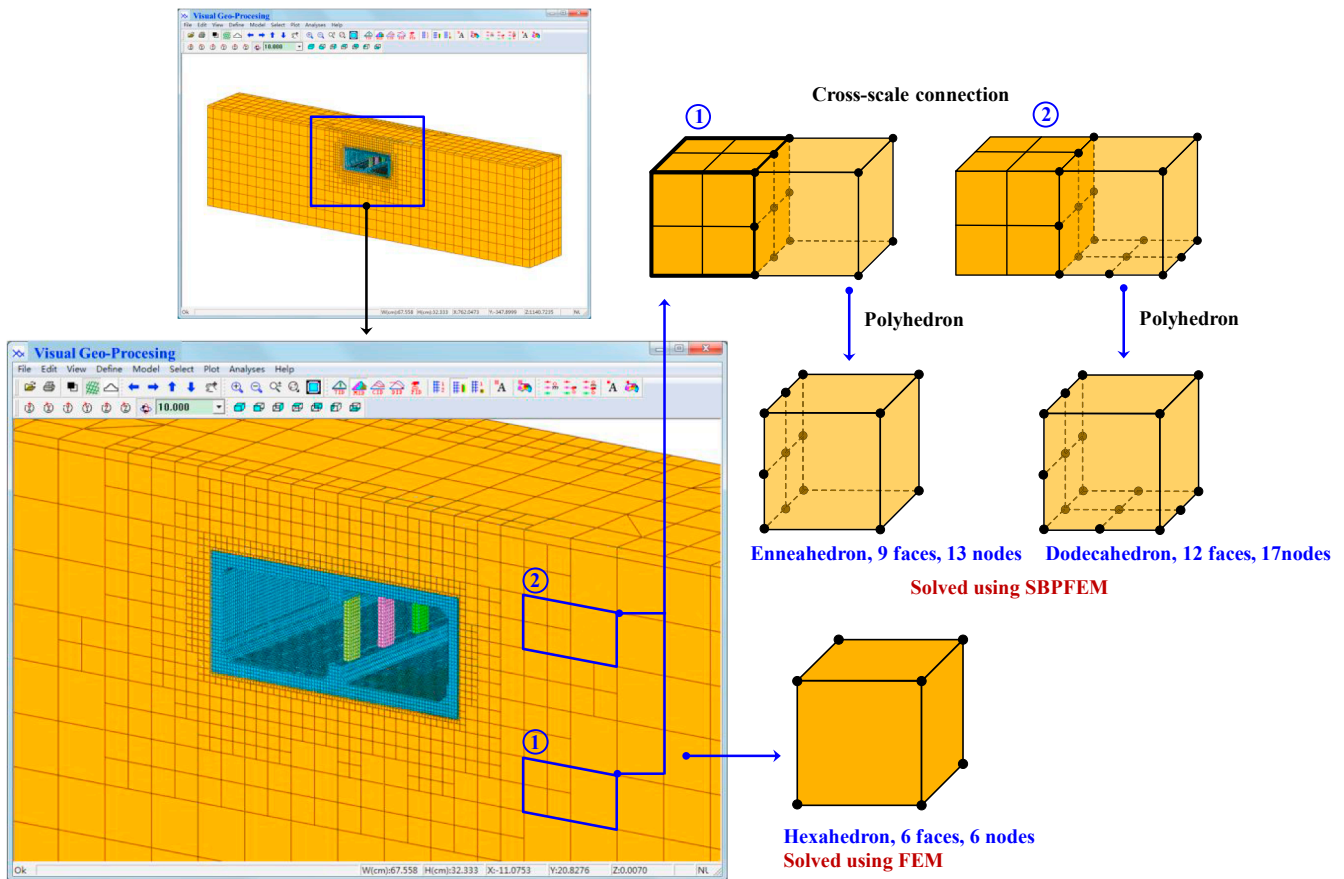


Fig. 3. Procedure for polyhedron visualization, editing and modification.

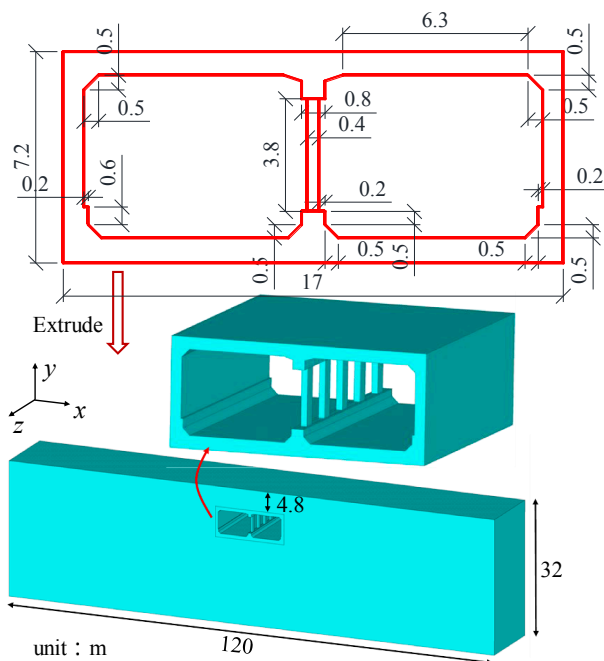


Fig. 4. Size description of the section and volume body (unit: m).

structures of the subway system, a fine mesh mesh can make the structural simulation more accurate. On the contrary, the stress sensitivity of the soil is lower, and the requirements for the size of the mesh for soil can be relaxed. However, due to the limitation of traditional element shapes, the encryption structure will inevitably lead to subdivision of soil

meshes, resulting in a significant increase in the overall computational cost.

The literature shows that fine analysis can more accurately reflect the mechanism of structural failure and structural seismic performance [17–19], both of which have emerged as a topic of much discussion and attention. However, the traditional approach to mesh partition suffers from multiple constraints and can require much manual intervention. For example, the discretization of complex geometry can account for about 80% of the total analysis time [20]. Moreover, due to the limitation of the traditional element shapes (e.g. hexahedrons and tetrahedrons), uniform small-scale refinement applied to the entire model can bring about an overwhelming amount of mesh points to be considered, thus making elasto-plastic analyses difficult and resource consuming. For a long time the trade off between mesh refinement and computational resource consumption has been difficult to reconcile. Therefore, there are few reports about refined damage propagation analysis for underground structures.

Qu [21,22] proposed an asymmetric interface element for handling the interface between solid structure and soil, thus opening a way to solve the problem of element size crossing at dissimilar interfaces. Additionally, the modeler approach the problem through several options, as shown in Fig. 1. Option 1 can be achieved using computer-aided engineering software (CAE, such as ANSYS and ABAQUS). In this paper ANSYS was used. Firstly, the plane geometry is imported to generate surface information in ANSYS. Then, according to the set transition level, the surface is cut into five parts (Fig. 1(1)). Through the discrete tool, the size of discrete elements is set for each surface, and finally, the graphical grid can be generated by clicking the mesh button. On the other hand, the mesh is difficult to generate directly using ANSYS for option 2. However, the mesh may be generated through the assistance of computer aided design (CAD) software. After drawing lines manually, the lines can be transformed into graphical mesh format (Fig. 1(2)) through custom programming. One such option is the manual/semi-automatic transition for the elements at the structure-soil interface. In

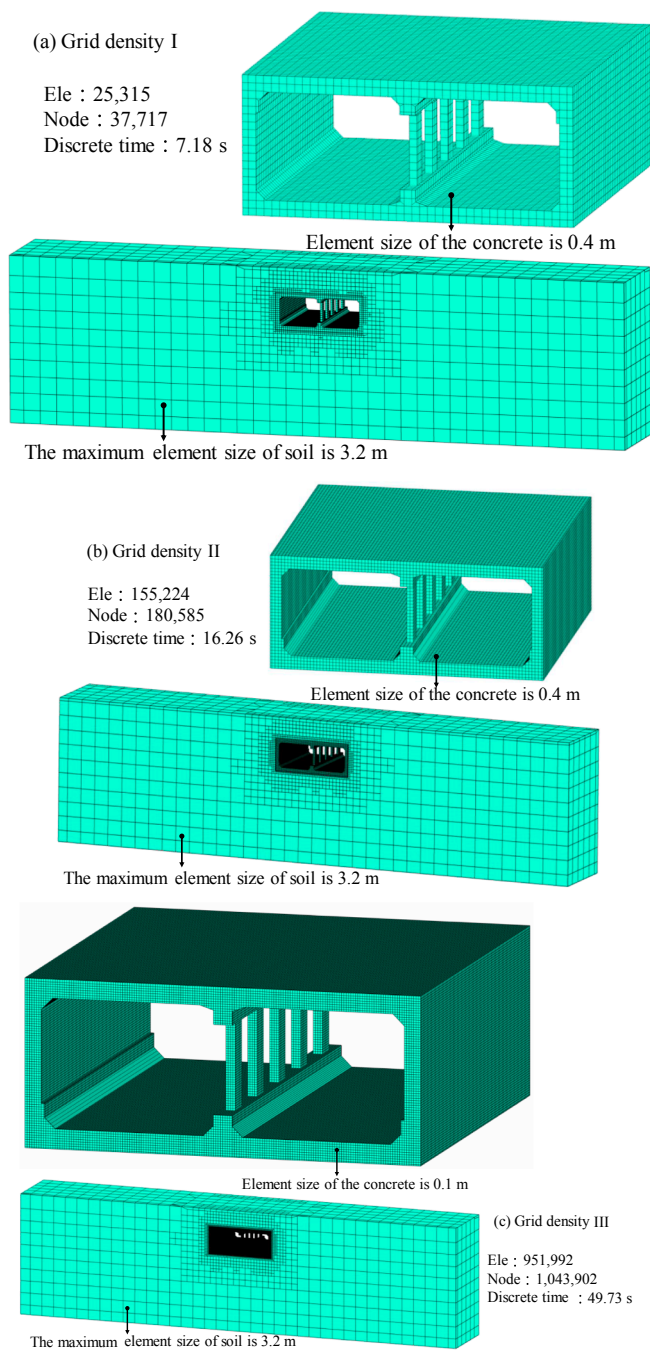


Fig. 5. Three different mesh size cases for the finite element model.

Table 3-1
Element proportions for three different mesh densities in the discretized model.

Case	Hexahedron	Polyhedron	Discrete time
Mesh density I	87.2%	12.8%	7.18 s
Mesh density II	91.3%	8.7%	16.26 s
Mesh density III	95.4%	4.6%	49.73 s

this option, the continuity of meshes between soil and structure is guaranteed and the spanning of element scale is achieved, while considerable manual intervention is still needed. Despite the benefits offered, the automation capabilities in this option requires further improvement. Furthermore, the multi-node constraint (MPC) method [16], which is mainly used to solve the constraint equations of interface nodes, has also been investigated by researchers, but its application scope and precision still need to be enhanced.

While increasing amounts of new and efficient techniques are emerging, there is still much room for improvement before they can be put to practice.

This paper combines the octree mesh discrete technique with the use of complex polyhedron in scaled boundary FEM [23,24], and considers some key factors to conduct refined damage propagation analysis. There is a need to emphasize that soil-structure interaction is highly complex and involves detailed considerations when constructing a model. Researchers have devoted considerable efforts to investigate the principles of soil-structure interactions, and many achievements have been accomplished. In his early work, Robertson, I.A. [25] investigated the effects of forced vertical vibration of a rigid circular disc on a semi-infinite elastic solid. The dynamic response of three-dimensional rigid surface foundations have been solved using BEM [26]. Luco, J.E. and Mita, A. [27] presented an alternative technique to obtain the dynamic response of a massless rigid circular foundation resting on a uniform elastic half-space. Their technique avoids the need to solve an independent set of mixed boundary value problems for the case of wave excitation, and eliminates the numerical problems associated with the singularity of the contact tractions along the perimeter of the foundations. Recently, Ahmadi, S.F. [28,29], Eskandari, M. [30,31], Shodja, H.M. [32] and Samea, P. [33] developed many methods to simulate the soil-structure interaction problems of bi-material full-spaces and transversely isotropic half-spaces. These works have contributed vital advances to solving the problem of soil-structure interaction, and provided an important theoretical basis for future researchers. In this paper, the viscoelasticity of the artificial boundary and the input method for the free wave field integrated in literature [34] are used to consider the interaction influence. Moreover, the constitutive model for soil elasto-plastic materials [35–37], the constitutive model for state-dependent contact surface [38], and the model for predicting plastic damage in concrete [39] are also considered to investigate the fine analysis of underground structures comprehensively. As a demonstration, a fine scale damage evolution analysis was conducted for the DaiKai subway station, which was once collapsed by a severe earthquake. Different mesh mesh sizes were employed to study the influence of mesh refinement on computation results. The practical potential of octree mesh discretization was further explored by processing geometric shapes at different complexity levels. This research work may provide a technical foundation and reference for accurately reproducing the structural failures of other large engineering structures.

2. Analysis platform

This paper describes the development of an elasto-plastic complex polyhedron element for use in scaled boundary FEM in the GEODYNA framework, which is a large-scale geotechnical software platform independently developed by [40,41]. The polyhedron element shape can be arbitrary (see in Fig. 2), thus bypassing the limitation of the conventional discrete elements (hexahedrons, pentahedrons and tetrahedrons). In doing so, the octree thought belonged to computer science could be applied to the efficient fine-scale meshing of complex geotechnical structure. In addition to the polyhedron element, the viscoelastic boundary, polygon interface element, polyhedron pre-processing visualization, editing and modification procedures are also developed (see Fig. 3). The amount of automation in the traditional discretization pre-processing step is significantly improved. All of the above was assembled together to create a cross-scale analysis platform for geotechnical engineering structures.

3. Fine-scale analysis program

3.1. Finite element analysis model

In this paper, the seismic-induced failure of the DaiKai subway station was taken as an example to conduct a detailed simulation of the evolution of damage during an earthquake. A representative cross-section and 3D model of the subway station is shown in Fig. 4. The design of the subway station is that of a closed frame concrete structure. The station is covered by a soil layer with a thickness of 4.8 m, and the depth from the top

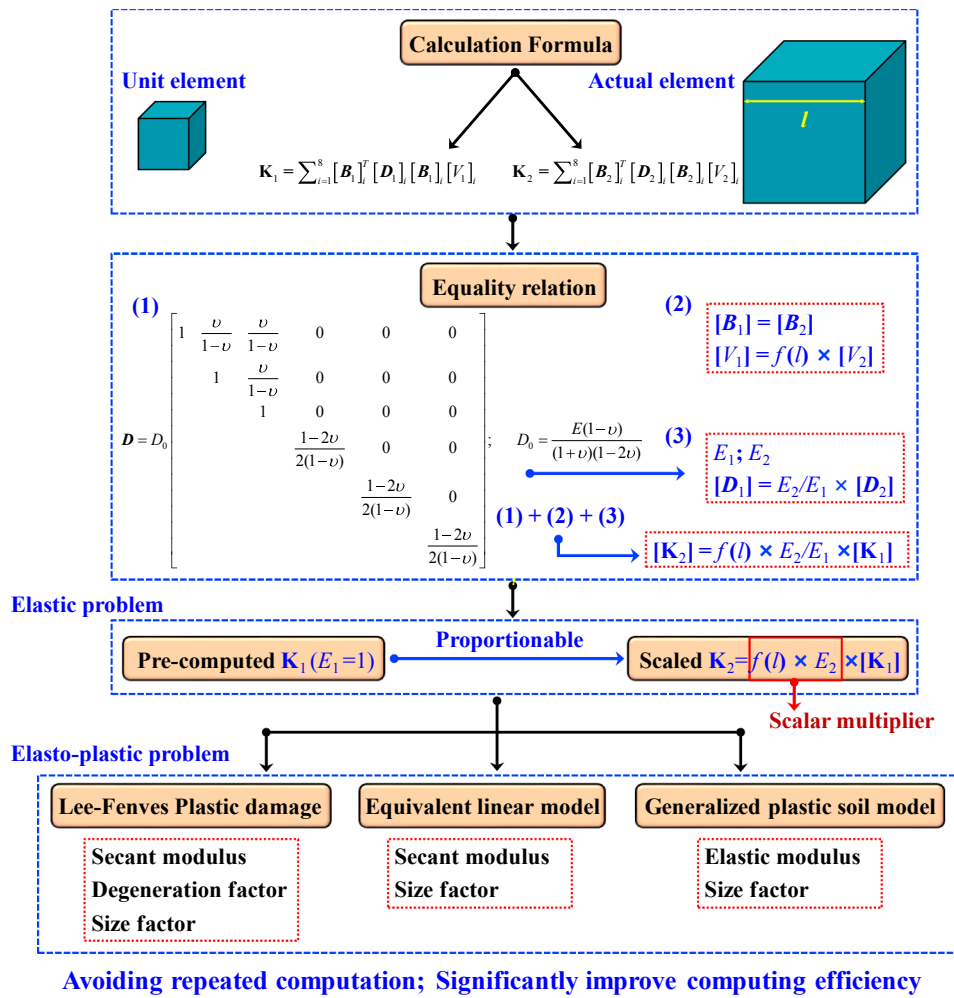


Fig. 6. Flow chart for using element similarity.

Table 3-2
Proportion of cubes in hexahedron population.

Case	Hexahedrons	
	Cube	Non-cube
Mesh density I	35.80%	64.20%
Mesh density II	51.28%	48.72%
Mesh density III	67.22%	32.78%

surface of the soil to the bottom surface is 32 m. The width of the simulation model is 120 m (about 7 times the station width). In addition, the cross-sectional area of the rectangular middle column supporting the station structure is $0.4 \times 1.0 \text{ m}^2$, and a 5-span interval is selected. According to the records, the DaiKai subway was not designed to be earthquake resistant. Therefore, during the Hanshin earthquake, the middle column within the station was severely damaged. As the two terminals of the roof were supported by rigid nodes, bending damage occurred in the upper roof once the middle column collapsed. Indeed, the maximum amount of damage sustained by the station during the earthquake occurred in the top plate. In order to reinforce against future damage, a M-shaped section [11,15] was implemented in the rebuilt station.

Three different mesh densities were used to reveal the effect of mesh size on the propagation of structural damage. The cross-scale model used for finite element analysis is shown in Fig. 5. The maximum size of the soil mesh size was set as 3.2 m, and the mesh size of concrete structure decreased from 0.4 m, 0.2 m, and finally to 0.1 m. Details of the three types of mesh densities are listed in Table 3-1. It can be seen from the table that the octree-generated

discrete elements are of high quality, with the proportions of the hexahedron (the cube and the cuboid) reaching about 90%. As mesh density increased, the proportion of hexahedrons also increased. Conventional elements were used in the FEM analysis, and the polyhedral elements were solved by semi-analytical scaled boundary FEM, which ensured high-precision analysis.

3.2. Element similarity

An element stiffness can be solved using Eqs. (3-1) and (3-2), where \mathbf{K} is the element stiffness matrix, Ω is domain of integration, \mathbf{B} is the strain-displacement transformation matrix, \mathbf{D} is the constitutive matrix, and dV is the volume of the element.

$$\mathbf{K} = \int_{\Omega} \mathbf{B}^T \mathbf{D} \mathbf{B} d\Omega = \int_{\Omega} \mathbf{B}^T \mathbf{D} \mathbf{B} dV \quad (3-1)$$

$$\mathbf{K} = \sum_{i=1}^8 \mathbf{B}_i^T \mathbf{D}_i \mathbf{B}_i V_i \quad (3-2)$$

$$\mathbf{D} = \mathbf{D}_0 \begin{bmatrix} 1 & \frac{\nu}{1-\nu} & \frac{\nu}{1-\nu} & 0 & 0 & 0 \\ & 1 & \frac{\nu}{1-\nu} & 0 & 0 & 0 \\ & & 1 & 0 & 0 & 0 \\ & & & \frac{1-2\nu}{2(1-\nu)} & 0 & 0 \\ & & & & \frac{1-2\nu}{2(1-\nu)} & 0 \\ & & & & & \frac{1-2\nu}{2(1-\nu)} \end{bmatrix}; \quad D_0 = \frac{E(1-\nu)}{(1+\nu)(1-2\nu)} \quad (3-3)$$

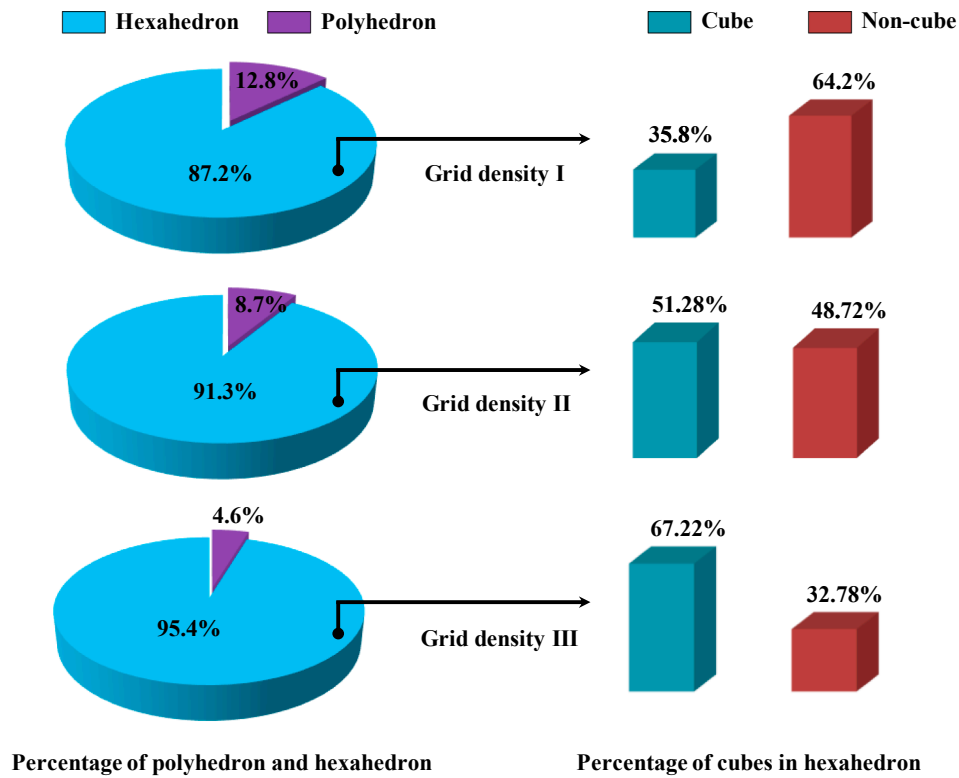


Fig. 7. Proportion of element times in the three different mesh densities mesh density.

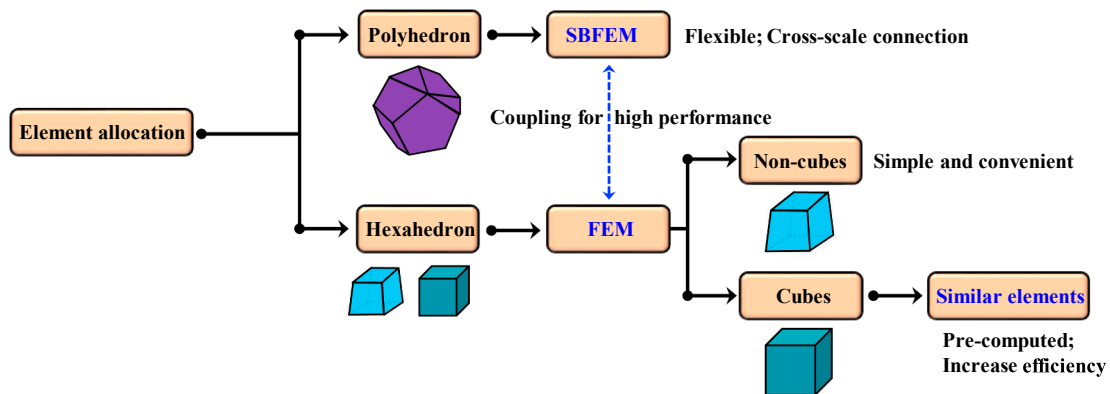


Fig. 8. Allocation of the computing element technology.

Matrix \mathbf{B} is only related to the interpolation shape function of the element, and is not related to element size. The constitutive matrix \mathbf{D} , as shown in Eq. (3-3), is determined by the elasticity modulus E and Poisson's ratio ν . D_0 is a scalar coefficient determined by E and ν , and i denotes the i^{th} Gaussian point. Here, an isoparametric element is used, and there are eight Gaussian points in total. For the elastic analysis of the same material, the modulus and Poisson's ratio are constant values, resulting in the values of matrix \mathbf{D} remaining constant. Therefore, the stiffness matrix \mathbf{K} is similar for cubes with different sizes but with same aspect ratios $f(l)$ (see in Fig. 6), and is thus proportional to element size. While the elastic modulus will change during the computation for elasto-plastic materials (such as soils), it is uncertain whether or not the similarity of stiffness matrices can be retained. Practical experiments suggest that this similarity can be preserved. The related principles are briefly discussed as follows:

(1) In the plastic damage model, the secant modulus is obtained through an iterative process, and thus the modulus can be obtained via the degeneration coefficient. As shown in Eq. (3-3), the

constitutive matrix is proportional to E . Assuming that $E = 1$, then the constitutive matrix \mathbf{D} can be treated as a constant, and the current stiffness matrix thus be obtained by multiplying the elastic modulus E_i evaluated in each Gaussian point i in the subsequent iteration. Therefore, the stiffness matrix can be obtained through a scaling factor in the plastic damage model.

- (2) For the same material, the Poisson's ratio ν can be considered as constant in the equivalent linear model. The strategy of elastic iteration is adopted on our developed program platform, namely, the elasticity modulus is always used for iteration in nonlinear iteration calculation. From Eq. (3-3), a conclusion can be drawn that the constitutive variable \mathbf{D} is proportional to the elastic modulus. Thus, the stiffness matrix can be solved using the proportional coefficient.
- (3) Similarly, the Poisson's ratio is not supposed to change in the generalized plastic model. The technique of elasticity modulus is employed in each iteration. In this manner, the stiffness matrix of different cubes can be computed directly via a proportional coefficient.

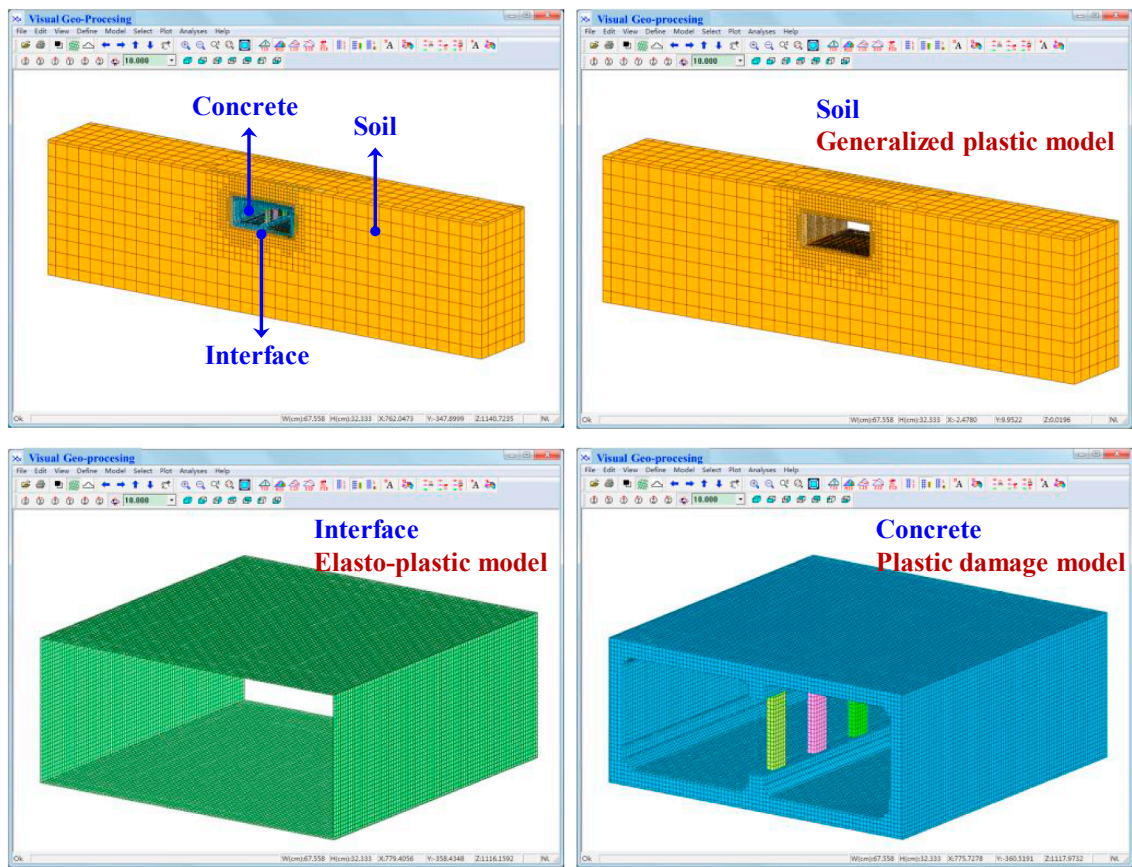


Fig. 9. Elasto-plastic material model assignment for the subway station and the surrounding soil.

Table 3-3
Parameters of the generalized plasticity model.

G_0	K_0	M_g	M_f	α_f	α_g	H_{u0}	H_{l0}	m_v
320	400	1.38	0.45	0.25	0.4	3000	900	0.20
m_l	m_s	β_0	β_1	γ_{DM}	r_d	γ_u	m_u	
0.40	0.20	25	0.01	70	20	5	0.40	

Table 3-4
Parameters of the generalized plastic interface model.

D_{s0}/kPa	D_{n0}/kPa	M_c	e_r	λ	$a/\text{kPa}^{0.5}$	b	c
1000	1500	0.88	0.0	0.091	224	0.06	3.0
γ_d	k_m	M_f	k	H_0/kPa	f_h	t/m	a
0.2	0.6	0.65	0.5	8500	2.0	0.1	0.65

Generally speaking, the use of element similarity can be extended to simulate the constitutive for model concrete plastic damage as well as the elasto-plastic constitutive model for soil, and derive the equivalent linear model, all of which will greatly improve the efficiency of damage simulation of underground structures. A flow chart of the use of element similarity is shown in Fig. 6.

Table 3-2 and Fig. 7 indicates another notable feature of the octree mesh that is the cubes account for a considerable percentage of hexahedrons. These cube elements are exactly the same except that the their sizes are in ratios of 2^n times of the unit cube. As the dimensions are proportionate to each other, the stiffness matrices of the elements are thus theoretically also similar and proportionate to each other. Thus, by simply computing and storing the parameters of a unit cube, the other cube elements, and thus the stiffness matrices of much of the model can be computed efficiently based on the unit cube.

As shown in Fig. 8, the small amount of polyhedrons are handled by

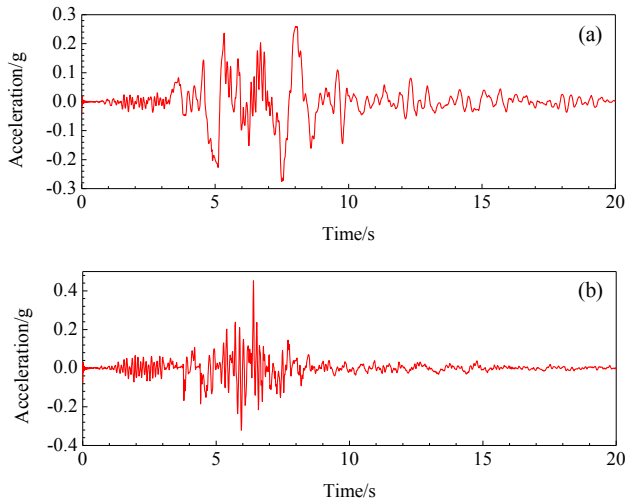


Fig. 10. Acceleration of the Kobe wave: (a) x-, (b) y-direction.

SBFEM, and the hexahedrons, which compose the bulk of the elements, are solved using FEM. However, unlike traditional FEM, the cubes are to be solved via the similar element technique.

3.3. Material parameters and ground motion input

In this paper, the soil is treated with a generalized plastic model [35–37], and the parameters are obtained according to the soil distribution, experimental and simulation data provided by the literature [6,9,15]. The constitutive model of the state-dependent interface [38] is used to simulate the soil-structure interaction (see Fig. 9). The model

Table 4-1
Information statistics of global refined and cross-scale meshes.

Size of concrete mesh	Type	Elements	Nodes
0.4 m	Global scale (G)	1,029,904	1,079,738
	Cross-scale (C)	29,318	37,917
	Reduction Ratio (G/C)	35.1	28.5
0.2 m	Global scale (G)	8,015,386	8,207,305
	Cross-scale (C)	155,224	180,585
	Reduction Ratio (G/C)	51.6	45.4
0.1 m	Global scale (G)	64,123,088	65,658,440
	Cross-scale (C)	951,992	1,043,902
	Reduction Ratio (G/C)	67.4	62.9

parameters are listed in Table 3-3 and Table 3-4. The concrete on the other hand is treated with a plastic damage model [39], and the model parameters are defined as follows: density $\rho = 2400 \text{ kg/m}^3$, elastic modulus $E = 32.5 \text{ GPa}$, Poisson's ratio $\nu = 0.2$, ultimate compressive strength $f_c = 25.6 \text{ MPa}$, ultimate tensile strength $f_t = 2.0 \text{ MPa}$.

For modeling the seismic response of the structure, a viscoelastic artificial boundary and the free wave field input method [34] is used. Fig. 10 shows the ground motion record observed in the Hanshin earthquake. The earthquake was implemented for 20 s with a time step of 0.005 s.

3.4. Results

Figs. A1–A3 show the overall damage distribution of the subway station computed using three mesh densities. Fig. A1 shows that when the mesh size of the concrete structure was 0.1 m, the structural damage was localized and the bands of damage were pronounced. There was also strong continuity in the damage distribution. Different levels of tensile and compressive damage occurred at the two ends of the columns, the top plate and the four corners. As the element size increased, the damage became less localized (Figs. A2 and A3). When the concrete scale was 0.2 m, the damage distribution became more diffuse. At an element size of 0.4 m, the structural damage became even more spread out, mainly due to the impact of element size. At the larger element sizes, when a portion of an element is destroyed, the simulation considered the entire element to be destroyed, thus effectively increasing the apparent damaged area. Thus, the results suggest that smaller mesh sizes can yield more accurate seismic responses, especially in regards to damage simulation.

Fig. A4 shows the deformation of concrete structure. The station roof was severely damaged by bending induced tensile stresses about 3 m away from the pillar location. As a result, the top plate collapsed and formed an M-shape. The resultant shape is in good agreement with the description of the station deformation after earthquake in the literature [11]. The damage results of the middle columns are compared to photographic records in Fig. A5. As seen in Fig. A5, a large number of the columns suffered severe crushing and tensile cracking, thus contributing to a loss of bearing capacity and ultimately causing the roof to collapse. In the simulation results, the damage factor in the ends of middle columns is close to 1.0, indicating a complete loss of bearing capacity and crushing in the columns. The lower part of the middle columns was also damaged greatly, further suggesting that the concrete structure is completely broken. A closer inspection of the column damage distribution reveals that the damage in the left of the columns was slightly larger than the right side. The slight disproportionate failure caused the columns to be toppled over. In summary, the failure mode of the middle columns obtained from the simulation results are consistent with the true seismic-induced damage. This case study demonstrates the practical applicability of the proposed method in the damage analysis of concrete structures under seismic excitation.

4. Application potential

The prior sections show in detail that the more refined the mesh is, the

more accurately the simulation can reflect the development of damage during the seismic excitation. Numerical simulations using adequately refined meshes is thus an effective way to accurately simulate the engineering catastrophe and reproduce the structural failure mode. Compared to traditional meshing methods, the proposed Octree-SBFEM benefits from several unique advantages. In particular, traditional modeling solutions face two major difficulties which are summarized as follows:

- (1) Traditional uniform scaled models are difficult to cross scale. Mesh refinement will result in a large number of elements that make it difficult to conduct an elasto-plastic analysis.

There is a wide difference in the nature of local vs global scale damage in large civil structures such as subway stations, large-scale bridges, high-rise buildings and other similar structures. Therefore, there is an urgency in the field to develop a computational model that can simultaneously simulate both local micro-damage and macro-behavior of the structure. Cross-scale analysis is an effective way to solve this problem. However, due to the constraints in element shape of isoparametric elements, it is difficult for the traditional modeling scheme to achieve high-performance, cross-scale modeling.

If a fine-scale discretization is adopted globally, the result will be a highly detailed mesh that will consume excessive amounts of computational resources. Considering the prior model as an example (parameters for all three cases listed in Table 4-1), one can observe that the mesh for the globally fine mesh (0.1 m) has a staggering amount of elements and nodes. The sheer number of components will have a total of 100 million degrees of freedom (10^8), which will be a daunting task for most computers to carry out. Practically, more than 90% of the geotechnical materials do not need such fine mesh density, and such mesh refinement will only return a few benefits in proportion to its massive computational cost. On the other hand, when using the cross-scale refinement method in this paper, the number of elements can be reduced 67.4 times, and the degree of freedom will be reduced to about 3 million. Furthermore, the mesh is still precise at key locations in the model, thus ensuring the accuracy of the simulation. Areas that are not influential on the results (e.g. the bulk of the soil) can be modeled using a sparser mesh to save computational cost. Therefore, the cross-scale refinement method optimizes the balance between accuracy and efficiency.

- (2) The hexahedral mesh has difficulty adapting to complex boundaries, and the labor cost is high, making it difficult to achieve automated discretization.

Automated hexahedral meshing means that the modelling program can automatically generate the hexahedral mesh. Most software currently supports mapping, dragging, sweeping and other functions to generate hexahedrons, but these functions are only applicable to simple models.

If complex situations such as soil stratification is considered (see Fig. B1), the task of mesh meshing through traditional methods will become highly difficult and labor intensive due to the amount of irregular boundaries. For complex 3D geometries, as shown in Fig. B2, when the two lines cross over, the conventional strategy of dragging and sweeping cannot be applied. Accurately modeling such a feature can take days of manual labor in cutting, simplification, block discretization, etc.

An alternative to model complex geometries with less manual involvement is to use automatic tetrahedral meshing. However, such an approach may result in poor performance if intermediate nodes (i.e. higher-order interpolation) is not used. Yet, once intermediate nodes are involved, another set of problems arise, including complications in processing, extended solving times, lower convergence rates, etc. Thus, the introduction of a program that can automatically generate hexahedral meshes will be beneficial for many researchers.

The two examples above can be easily and efficiently handled via the octree cross-scale scheme. As shown in Fig. B3 and Fig. B4, the

meshing can be completed in a short time, and the ratio of hexahedron reached approximately 90%. Furthermore, the mesh density can be adjusted by simply redefining the maximum and minimum mesh size. These two additional examples further demonstrate how the use of octree cross-scaling for meshing can save in computational and labor costs. The proposed method lays the foundation for further work in automated discretization.

5. Conclusion

This paper presented the integration of semi-analytical scaled boundary polyhedral element (SBFEM) with the efficient octree-based discretization method to eliminate restrictions on element shapes and greatly increase solution speeds for fine scale analysis. The integration gives structural engineers a streamlined platform for efficient yet accurate modeling and solving results for complex geometries. A demonstration was performed by using the proposed method for the fine-scale analysis of the DaiKai subway station under seismic excitation. The computation results obtained from the method are in good agreement with the actual seismic damage shown in photographs. The paper also discussed the applications and development potential of the method. Three preliminary conclusions about the method can be drawn as follows:

- (1) With mesh refinement, the damage distribution of the DaiKai subway was localized and continuous, indicating that the fine-scale analysis can more accurately reflect the structural seismic response and damage propagation. The results suggests that in a broad sense, the use of refined meshes may be a necessary approach for accurate simulation of earthquake damage.
- (2) The use of a globally fine mesh will generate an unnecessarily large number of elements and nodes that will waste computational resources. The increased number of components also makes it difficult to perform elasto-plastic analysis. On the other hand, the octree-based, cross-scale modeling is a novel approach to drastically reduce computational costs while maintaining the required amount of accuracy. In the examples shown in prior sections, only a few minutes was needed for the method to automatically generate a hybrid mesh (fine scale at key locations, coarse at unimportant

- locations) for complex geometries. The method is especially useful at handling interfaces between uneven layers of dissimilar materials. The method has strong processing capabilities and potential for the mesh generation of arbitrary three-dimensional geometries.
- (3) Solver efficiency is another bottleneck for simulation speeds. According to the case study in the paper, 90% of the model was composed of conventional elements generated by the octree-based. Within this population of elements, more than 60% were cubic and were geometrically similar. With the similar geometry, the parameter matrices (i.e. stiffness matrix, mass matrix and damping matrix) among the elements also become similar and scalable. Thus, from one unit cubic element, the parameters of all other cubic elements can be derived. This “nonlinear similar element” (NSE) method avoids considerable repeated computations, and significantly improves the solution efficiency. Additionally, the strategy of coupling SBFEM-FEM will fully leverage the advantages of two methods. Furthermore, the example applications shown in the paper demonstrated that coupled SBFEM-FEM and NSE markedly optimized the computational performance. Approximately 50% of the computational time was reduced in the DaiKai simulation. The proposed method has strong potential for simulating seismic attack of complex systems such as water conservation facilities, long-span bridges and nuclear power plants.

While the work detailed in this paper demonstrated the feasibility, efficiency and potential of the method, there are certain aspects that were neglected. For example, the simulation would be even more accurate by considering experimentally obtained values of the actual soil layer, the consideration of steel mesh etc. The inclusion of these factors will be explored and discussed in the future development of the method.

Acknowledgements

This work was supported by National Key R&D Program of China (2017YFC0404904) and the National Natural Science Foundation of China (Grant Nos. 51779034, 51608095). And the Fundamental Research Funds for the Central Universities (Grant No. DUT17ZD219).

Appendix

A. Results of DaiKai simulation

See Figs. A1–A5.

A. Results of DaiKai simulation

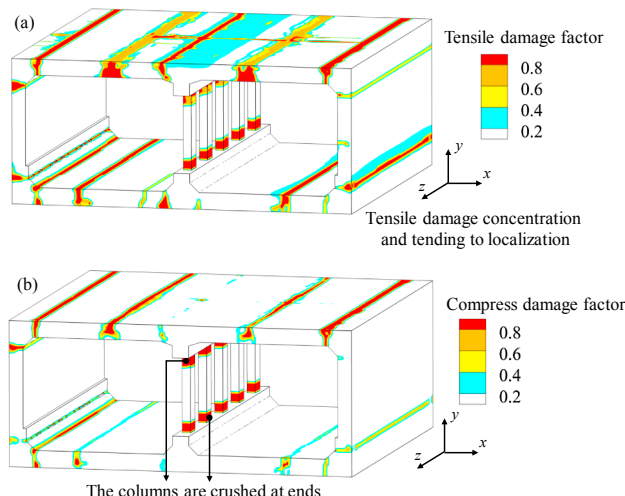


Fig. A1. Global diagram of damage distribution (mesh size 0.1 m for concrete).

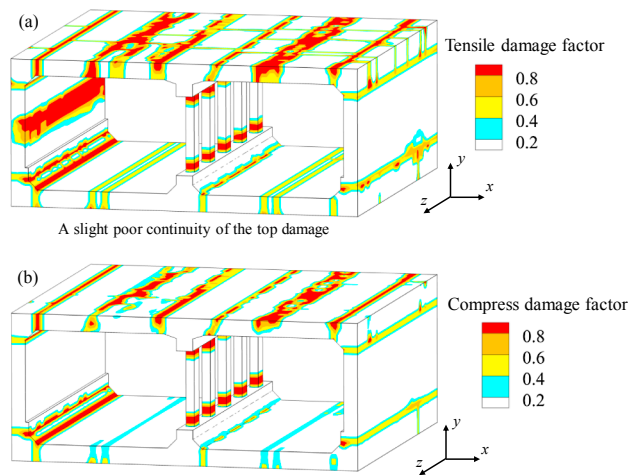


Fig. A2. Global diagram of damage distribution (mesh size 0.2 m for concrete).

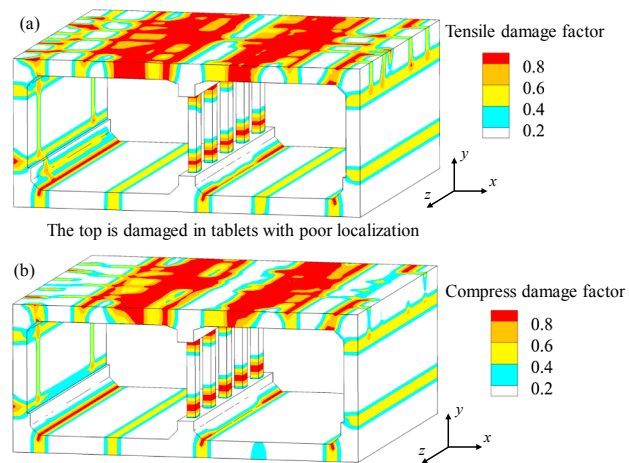


Fig. A3. Global diagram of damage distribution (mesh size 0.4 m for concrete).

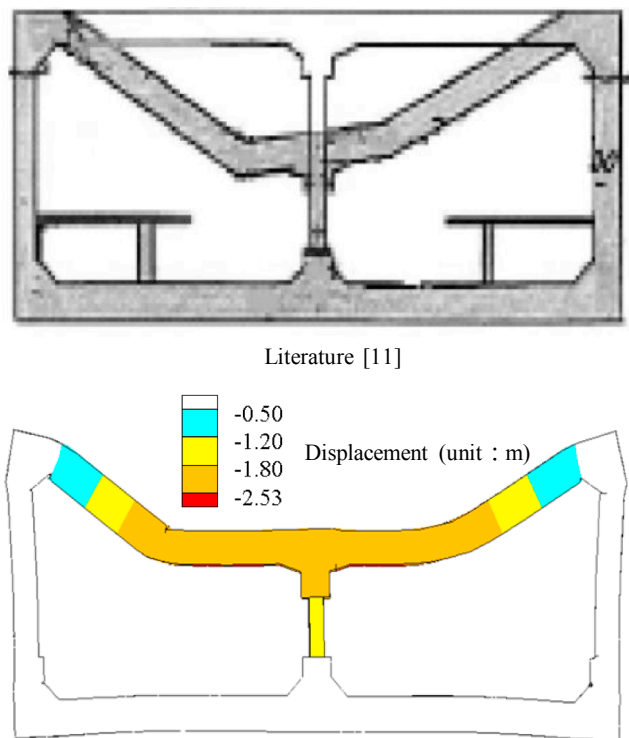


Fig. A4. Deformed shape of the damaged subway station (cross section).

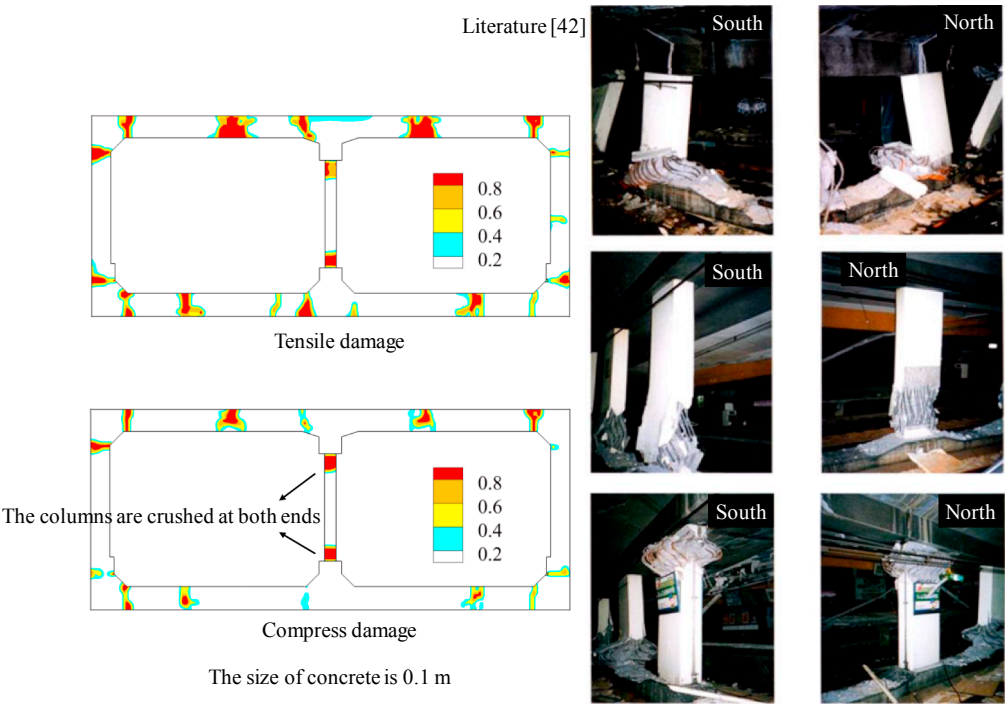


Fig. A5. Comparison between the damage distribution and the actual seismic damage [42].

B. Example of applying coupled SBFEM-FEM

See Figs. B1–B6.

B. Example of applying coupled SBFEM-FEM

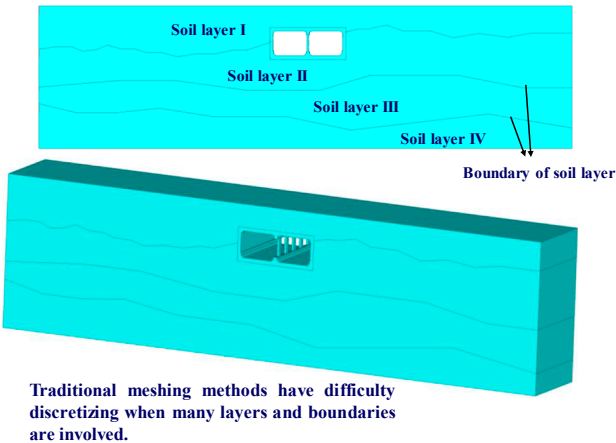
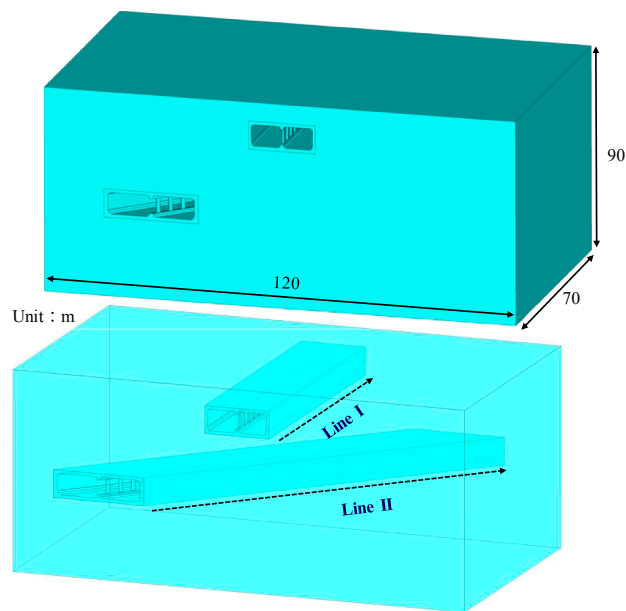


Fig. B1. Situation in which the boundaries of different soil layers are considered.



When two lines cross over in 3D space, traditional modeling methods do not allow dragging or automated discretization. Such a situation will be extremely difficult to handle using conventional means.

Fig. B2. A portion of the metro infrastructure where two subway lines interleave each other.

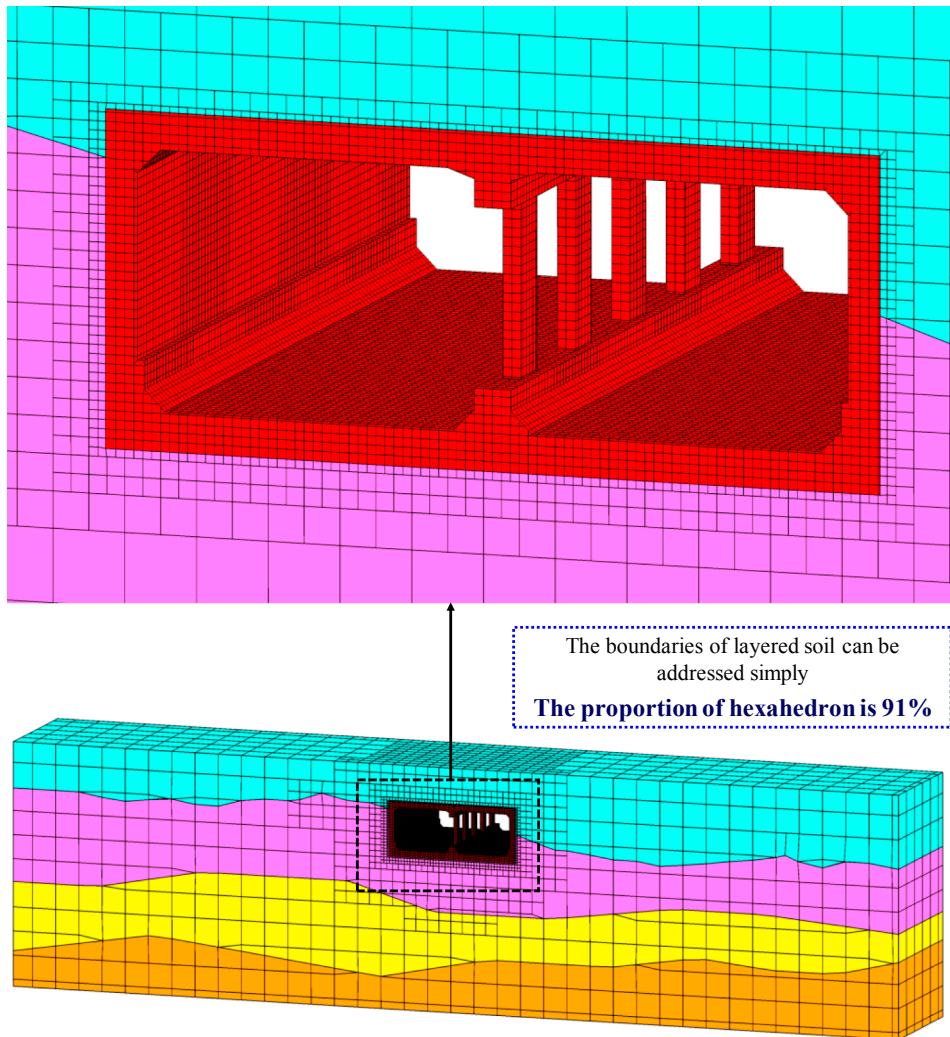


Fig. B3. Discretization of the metro station with layered soil using octree.

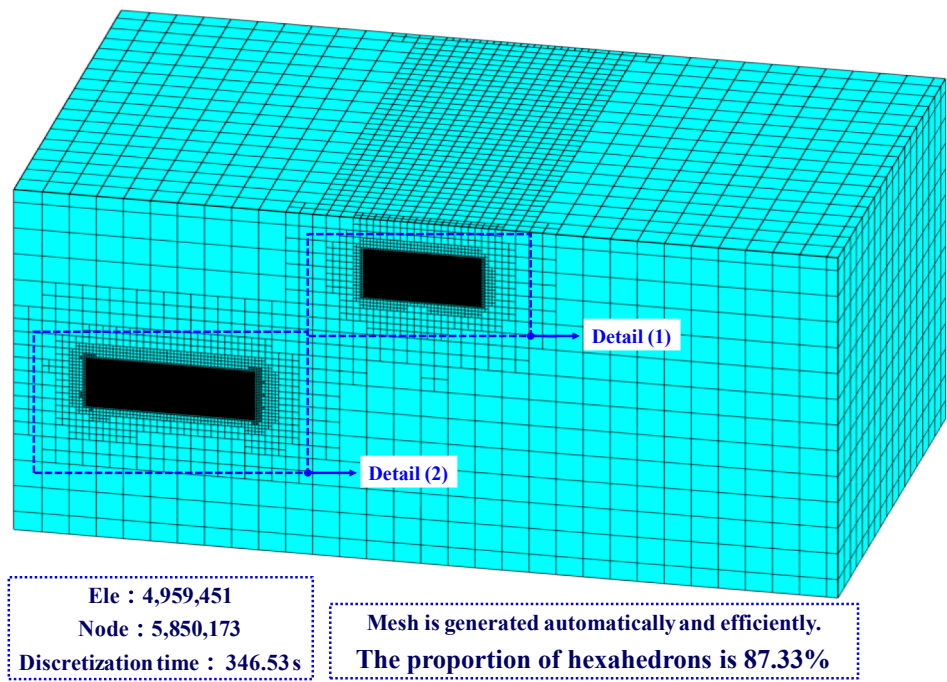


Fig. B4. Discretization for interleaving subway circuit using octree.

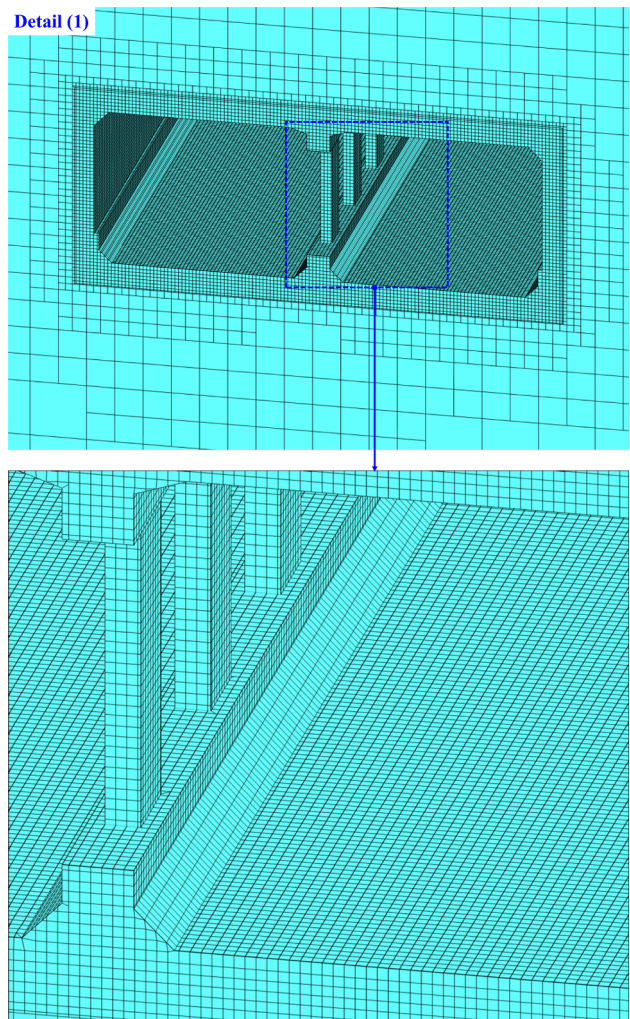


Fig. B5. Partial detail (1) for discretization for interleaving subway circuit using octree.

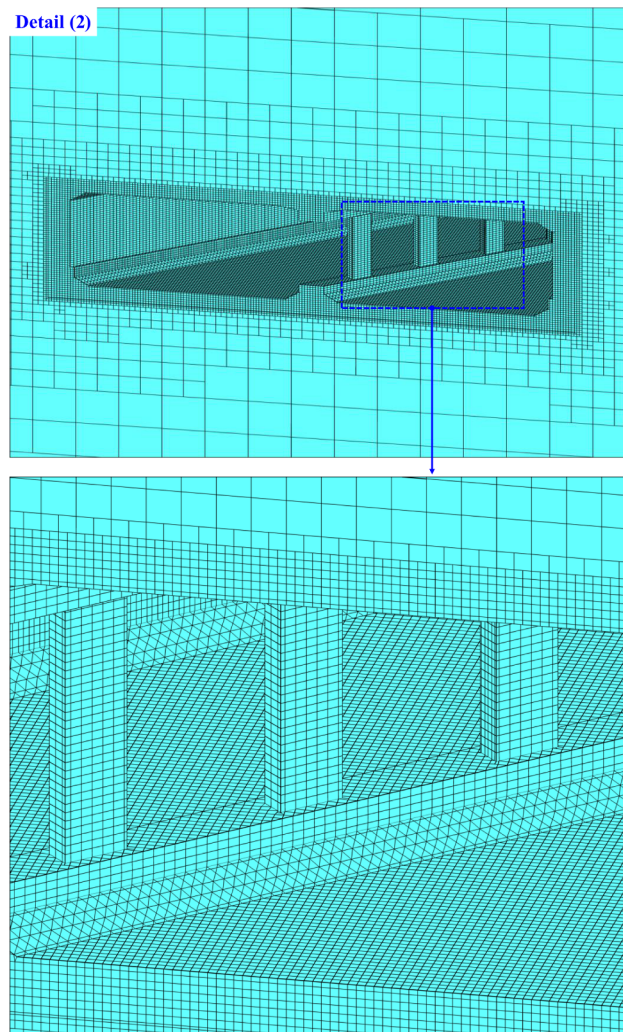


Fig. B6. Partial detail (2) for discretization for interleaving subway circuit using octree.

References

- [1] Lin Zhang. Research on the function of orbital transportation to the development of city. Shanghai: Shanghai Normal University; 2010. (in Chinese).
- [2] Guo-Xing Chen, Xi Zuo, Hai-Yang Zhuang, et al. Contrast analysis of numerical simulation of subway tunnel earthquake response with test results. *J Nat Disasters* 2007;16(6):81–7. (in Chinese).
- [3] Lei Chen, Guo-Xing Chen, Hui Long. 3D refined nonlinear finite element analysis of intersecting metro tunnels under near-field ground motion. *Rock Soil Mech* 2010;31(12). 3971–3976 + 3983 (in Chinese).
- [4] Guo-Xing Chen, Xi Zuo, Zhi-Hua Wang, et al. Large scale shaking table test study of the dynamic damage behavior of subway station structures in liquefiable foundation under near-fault and far-field ground motions. *China Civ Eng J* 2010;43(12):120–6. (in Chinese).
- [5] Uenishi K, Sakurai S. Characteristic of the vertical seismic waves associated with the 1995 Hyogo-ken Nanbu (Kobe), Japan earthquake estimated from the failure of the Daikai Underground Station. *Earthquake Eng Struct Dyn* 2000;29(6):813–22.
- [6] Bing-Zheng Cao, Qi-Feng Luo, Shuo Ma, et al. Seismic response analysis of Dakai subway station in Hyogoken-nanbu earthquake. *Earthquake Eng Eng Vib* 2002;22(4):102–7. (in Chinese).
- [7] Huo H, Bobet A, Fernández G, et al. Load transfer mechanisms between underground structure and surround ground: evaluation of the failure of the Daikai station. *J Geotech Geoenviron Eng* 2005;131(12):1522–33.
- [8] Xiang-Qing Liu. Research on analysis method and experimental study of seismic response of underground subway structures. Beijing: Tsinghua University; 2008. (in Chinese).
- [9] Chao Sun. Study on seismic capability and analysis method of underground subway structures. Harbin: Institute of Engineering Mechanics, China Earthquake Administration; 2009. (in Chinese).
- [10] Liu Ru-Shan Wu, Xiu-Li Yu-Bin, Du. Numerical simulation analysis on earthquake damage of underground structure with fiber model. *J Beijing Univ Technol* 2010;36(11):1488–95. (in Chinese).
- [11] Yi Huan, Qin Fang, Li Chen, et al. 3D nonlinear damage analysis of metro-station structures under strong seismic loading. *J Beijing Univ Technol* 2011;37(6):852–62. (in Chinese).
- [12] Jian-Min Zhang, Gang Wang. Large post-liquefaction deformation of sand, part I: physical mechanism, constitutive description and numerical algorithm. *Acta Geotech* 2012;7(2):69–113.
- [13] Yin Gu, Hua Zhong, Wei-Dong Zhuo. Analysis of dynamic interaction between soil and large subway station structure under seismic excitation based on 3d model. *Chin J Rock Mech Eng* 2013;32(11):2290–9. (in Chinese).
- [14] De-Chun Lu, Xin Wang, Lei Luo. Research on the seismic responses of underground structures considering the soil and structure contact. *J Disaster Prevent Mitigation Eng* 2017;37(02):177–86. (in Chinese).
- [15] Xiu-Li Du, Gang Wang, De-Chun Lu. Earthquake damage mechanism analysis of Dakai metro station by Kobe earthquake. *J Disaster Prevent Mitigation Eng* 2016;36(2):165–71. (in Chinese).
- [16] Xiu-Li Du, Chao Ma, De-Chun Lu, et al. Collapse simulation and failure mechanism analysis of the Daikai subway station under seismic loads. *China Civ Eng J* 2017;50(1):53–62. (in Chinese).
- [17] Mi Zhou, Jun-Jie Wang, Wan-Cheng Yuan, et al. Seismic performance assessment of liede bridge based on detailed finite element analysis. *J Tongji Univ (Nat Sci)* 2008;36(02):143–8. (in Chinese).
- [18] Ke-Yang Chen. Mesh generation and its accuracy and calculation analysis. *Inland Earthquake* 2011;25(01):12–20. (in Chinese).
- [19] Xin-Huang Zou, Si-Wen Xu. Refined finite element model modeling method of connecting angle sheet metal structure of large civil aircraft fuselage frame and the stringer. *China Sci Technol Inf* 2016;15:83–5. (in Chinese).
- [20] Bazilevs Y, Calo VM, Cottrell JA, et al. Isogeometric analysis using T-splines. *Comput Methods Appl Mech Eng* 2010;199(5–8):229–63.
- [21] Yong-Qian Qu, De-Gao Zou, Xian-Jing Kong, et al. A flexible various-scale approach for soil-structure interaction and its application in seismic damage analysis of the underground structure of nuclear power plants. *Sci China Technol Sci* 2018;61(7):1092–106.
- [22] Yong-Qian Qu, De-Gao Zou, Xian-Jing Kong, et al. A novel interface element with

- asymmetric nodes and its application on concrete-faced rockfill dam. *Comput Geotech* 2017;85:103–16.
- [23] Chen K, Zou D, Kong X, et al. A novel nonlinear solution for the polygon scaled boundary finite element method and its application to geotechnical structures. *Comput Geotech* 2017;82:201–10.
- [24] Chen K, Zou D, Kong X, et al. An efficient nonlinear octree SBFEM and its application to complicated geotechnical structures. *Comput Geotech* 2018;96:226–45.
- [25] Robertson IA. Forced vertical vibration of a rigid circular disc on a semi-infinite elastic solid. *Mathematical proceedings of the Cambridge philosophical society*. Cambridge University Press; 1966. p. 547–53.
- [26] Karabalis DL, Beskos DE. Dynamic response of 3-D rigid surface foundations by time domain boundary element method. *Earthquake Eng Struct Dyn* 1984;12(1):73–93.
- [27] Luco JE, Mita A. Response of a circular foundation on a uniform half-space to elastic waves. *Earthquake Eng Struct Dyn* 1987;15(1):105–18.
- [28] Ahmadi SF, Eskandari M. Vibration analysis of a rigid circular disk embedded in a transversely isotropic solid. *J Eng Mech* 2013;140(7):04014048.
- [29] Ahmadi SF, Eskandari M. Rocking rotation of a rigid disk embedded in a transversely isotropic half-space. *Civ Eng Infrastruct J* 2014;47(1):125–38.
- [30] Eskandari M, Shodja HM, Ahmadi SF. Lateral translation of an inextensible circular membrane embedded in a transversely isotropic half-space. *Eur J Mech-A/Solids* 2013;39:134–43.
- [31] Eskandari M, Ahmadi SF, Khazaeli S. Dynamic analysis of a rigid circular foundation on a transversely isotropic half-space under a buried inclined time-harmonic load. *Soil Dyn Earthquake Eng* 2014;63:184–92.
- [32] Shodja HM, Ahmadi SF, Eskandari M. Boussinesq indentation of a transversely isotropic half-space reinforced by a buried inextensible membrane. *Appl Math Model* 2014;38(7–8):2163–72.
- [33] Ahmadi SF, Samea P, Eskandari M. Axisymmetric response of a bi-material full-space reinforced by an interfacial thin film. *Int J Solids Struct* 2016;90:251–60.
- [34] Chen-Guang Zhou. Research on the mechanism of seismic wave input about high rockfill dams. Dalian University of Technology; 2009. (in Chinese).
- [35] Pastor M, Zienkiewicz OC, Leung KH. Simple model for transient soil loading in earthquake analysis. II. Non-associative models for sands. *Int J Numer Anal Meth Geomech* 1985;9(5):477–98.
- [36] Mroz Z, Zienkiewicz OC. Uniform formulation of constitutive equations for clays and sands. *Mech Eng Mater* 1984;12:415–49.
- [37] Hua-Bei Liu. Unified sand modeling using associated or non-associated flow rule. *Mech Res Commun* 2013;50:63–70.
- [38] Jing-Mao Liu, De-Gao Zou, Xian-Jing Kong. A three-dimensional state-dependent model of soil-structure interface for monotonic and cyclic loadings. *Comput Geotech* 2014;61:166–77.
- [39] Xiang Yu, Xian-Jing Kong, De-Gao Zou, et al. Linear elastic and plastic-damage analyses of a concrete cut-off wall constructed in deep overburden. *Comput Geotech* 2015;69:462–73.
- [40] De-Gao Zou, Kai Chen, Xian-Jing Kong, et al. An enhanced octree polyhedral scaled boundary finite element method and its applications in structure analysis. *Eng Anal Boundary Elem* 2017;84:87–107.
- [41] Kai Chen, De-Gao Zou, Xian-Jing Kong, et al. An efficient nonlinear octree SBFEM and its application to complicated geotechnical structures. *Comput Geotech* 2018;96:226–45.
- [42] Xiu-Li Du, Yang Li, Cheng-Shun Xu, et al. Review on damage causes and disaster mechanism of Daikai subway station during 1995 Osaka-Kobe Earthquake. *China J Geotech Eng* 2018;40(2):223–36. (in Chinese).